www.ijprems.com
editor@ijprems.com

INTERNATIONAL JOURNAL OF PROGRESSIVE RESEARCH IN ENGINEERING MANAGEMENT AND SCIENCE (IJPREMS)

Vol. 02, Issue 10, October 2022, pp : 05-16

e-ISSN : 2583-1062

Impact Factor : 2.265

INFLUENCE OF TEXTURE LOCATION ON THE STATIC PERFORMANCE CHARACTERISTICS OF HYDRODYNAMIC JOURNAL BEARING SYSTEM

Harmeet Singh[1], Arjan Singh[2]

[1]M. Tech Student, Department of Mechanical Engineering, Sri Sai College of Engineering & Technology, Pathankot

[2]Associate Professor, Department of Mechanical Engineering, Sri Sai College of Engineering & Technology, Pathankot, India

[1]Corresponding Author - Hrmitxng@gmail.com

ABSTRACT

The surface textures can improve the performance characteristics of journal bearing and thus a budding attention is given to the study of textured hydrodynamic journal bearings. The use of different texture shapes and at different locations is an effective approach to improve the performance characteristics of journal bearings. The present study investigates the influence of texture location on the static performance characteristics of hydrodynamic journal bearing. A numerical modelling is used to analyze the effect of spherical texture location on the static performance characteristics of a hydrodynamic journal bearing. The theoretical results show that the most important characteristics can be improved through an appropriate arrangement of the texture location on the bearing surface. The most optimum results are obtained when the textures are created in the pressure build-up zone of 125° to 285 °on the bearing surface.

1. INTRODUCTION

Tribology is a study of friction, wear, lubrication, and contact mechanics. It helps in understanding the surface interactions and to propose solutions for essential problems. The tribological applications range from industrial machinery to microscopic applications. The hydrodynamic bearings are frequently used in wide range of applications and mechanisms since long. The random roughness in hydrodynamic bearings may be introduced due to the presence of dust, additives in the lubricant and wear. The roughness may be random or deterministic in nature. The deterministic roughness is known as surface texture can be introduced deliberately on the bearings with the help of micro fabrication techniques. Surface texturing is claiming progressively more attention and is expected to be an important component in future bearing structure design as demonstrated by the authors [1]. Tonder [2] pointed out that the introduction of a series of dimples at inlet of a sliding surface can generate extra pressure and thus support higher load. Kovalchenko et al. [3] claimed that laser texturing expanded the contact parameters in terms of load and speed for hydrodynamic lubrication. Siripuram and Stephens [4] numerically studied the microasperities effects with different shapes in sliding surface lubrication. They concluded that the minimum coefficient of friction for all shapes is found to occur at an asperity area fraction of 0.2 for positive asperities and 0.7 for negative asperities. Some other studies [5-11] established that the surface texture geometry such as texture depth, width, number of textures, and location of textures influence the bearing performance. Arghir et al. [12] shown that Navier–Stokes equations are inadequate to predict pressure build-up with the presence of macro-roughness as inertia effects can be more important. This finding was confirmed later by Sahlin et al. [13]. De Kraker et al. [14], used the Reynolds equation to study the effects of texture and is valid if dimple depth is greater than minimum film thickness of the lubricant in the fluid film lubrication. Cupillard et al. [15] found that the mechanism of pressure build-up in a convergent gap between two sliding surfaces due to texture is similar to that obtained with convergence ratio variation for smooth surfaces. The same author [16] found that there is an optimal texture depth, greater than the critical depth, which gives the maximum load carrying capacity. Buscaglia et al. [17, 18] shown that full texturing has a negative impact on both hydrodynamic lift and viscous friction. Dobrica et al. [19] conclude that: Full texturing is unable to generate hydrodynamic lift in parallel sliders, except when the dimples are placed at the slider inlet. Attempts were made in several studies to determine the optimal texturing parameters that would minimize friction or maximize the load carrying capacity. Singh and Awasthi [20] concluded that the location of textures on the bearing surface plays an important role in improving the performance characteristics of journal bearing. Also, they concluded that the partial texturing can improve the overall performance of the journal bearing if the textures are placed in the pressure build-up region of 126°-286° in circumferential direction and over the entire axial direction [21]. Singh & Awasthi studied the influence of texture shapes on the performance parameters of textured journal bearings. Recently, Singh & Awasthi studied dynamic stability of textured journal bearing [22].

In the present work, deterministic spherical texture is used to study the influence of textures location on the bearing surface. To study the texture location effect on the static performance characteristics of journal bearing, 4

www.ijprems.com
editor@ijprems.com

INTERNATIONAL JOURNAL OF PROGRESSIVE RESEARCH IN ENGINEERING MANAGEMENT AND SCIENCE (IJPREMS)

Vol. 02, Issue 10, October 2022, pp : 05-16

e-ISSN : 2583-1062

Impact Factor : 2.265

spherical textures are created in the axial direction and 7 spherical textures are created in the circumferential direction. Then optimum texture distribution location is calculated using a numerical FEM technique. The simulated results of partially textured bearing are then compared with smooth bearing to have the better insight of texture distribution on the bearing surface. Figure 1 shows the distribution of spherical textures over the entire bearing (fully textured bearing)

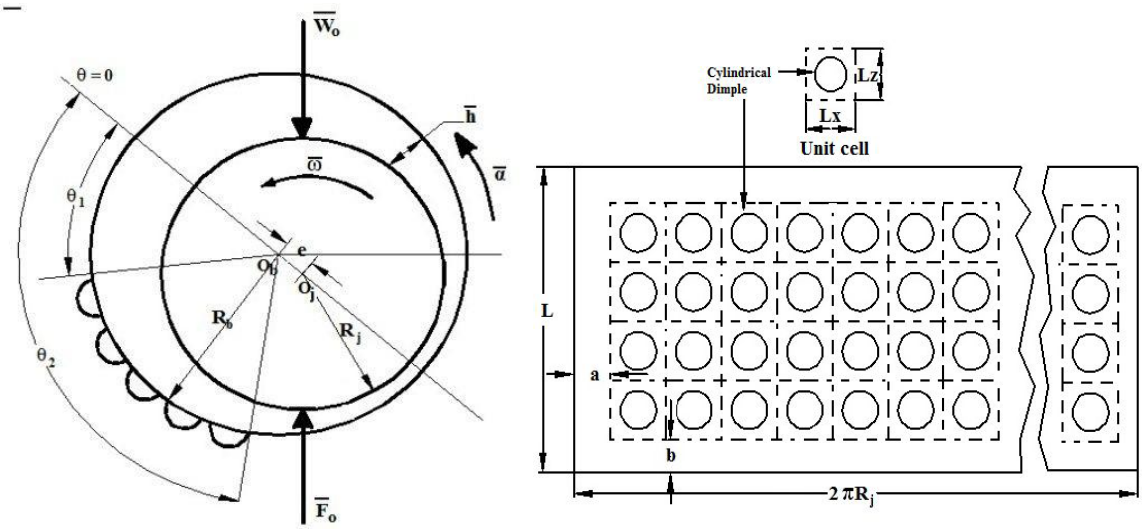

Fig.1 Full-textured journal bearing geometry

2. METHODOLOGY

2.1 Governing Equation

The governing Reynold's equation in dimensionless form of a journal bearing when the flow of lubricant is laminar, isoviscous and Newtonian in the convergent area of a journal and bearing can be written as [20]

$$\frac{\partial}{\partial\alpha}\left(\bar{h}^3\,\bar{F}_2\,\frac{\partial\bar{p}}{\partial\alpha}\right)+\frac{\partial}{\partial\beta}\left(\bar{h}^3\,\bar{F}_2\,\frac{\partial\bar{p}}{\partial\beta}\right)=\Omega\left[\frac{\partial}{\partial\alpha}\left\{\left(1-\frac{\bar{F}_1}{\bar{F}_0}\right)\bar{h}\right\}\right]+\frac{d\bar{h}}{d\bar{\tau}} \quad (1)$$

Where $\bar{F}_0$, $\bar{F}_1$ and $\bar{F}_2$ are cross apparent viscosity integrals and calculated as

$$\bar{F}_0=\int_0^1\frac{1}{\bar{\mu}}\,d\bar{Z},\quad \bar{F}_1=\int_0^1\frac{\bar{Z}}{\bar{\mu}}\,d\bar{Z},\quad \bar{F}_2=\int_0^1\frac{\bar{Z}}{\bar{\mu}}\left(\bar{Z}-\frac{\bar{F}_1}{\bar{F}_0}\right)d\bar{Z}$$

The Reynolds equation (1) is solved using FEM to study the influence of texture location on the bearing surface.

2.2. Fluid- film thickness ($\bar{h}$)

In dimensionless form, the fluid-film thickness having spherical textures on the bearing surface can be written as

$$\left.\begin{array}{ll}\bar{h}_d=\left[\left(\frac{\bar{h}_p}{2}+\frac{\bar{r}_p{}^2}{2\bar{h}_p}\right)^2-\bar{r}_p{}^2\left(\bar{x}_l{}^2+\bar{z}_l{}^2\right)\right]^{1/2}-\left[\frac{\bar{r}_p{}^2}{2\bar{h}_p}-\frac{\bar{h}_p}{2}\right] & r<\bar{r}_p\\ 0 & r\geq\bar{r}_p\end{array}\right\} \quad (2)$$

.

$\bar{h}_d$ =Dimple depth, $\overline{X}_j=\varepsilon\sin\phi$, $\overline{Z}_j=\varepsilon\cos\phi$

The eccentricity ratio (ε) is expressed as

$$\varepsilon=\sqrt{\bar{X}_j{}^2+\bar{Z}_j{}^2} \quad (3)$$

2.3. Finite element formulation

The fluid-flow domain is discretized using 4-noded quadrilateral iso-parametric elements. The pressure of the lubricant is considered to be linear over an element and can be expressed as [20]

$$\bar{P}=\sum_{j=1}^{n_e}\bar{P}_j\,N_j \quad (4)$$

Where Nj is the element shape function and ne is the number of nodes per element of two dimensional flow-field discretized solution domain. By applying Galarkin's FEM approach, the global system of equation in algebric form is expressed as [20]:

www.ijprems.com
editor@ijprems.com

INTERNATIONAL JOURNAL OF PROGRESSIVE RESEARCH IN ENGINEERING MANAGEMENT AND SCIENCE (IJPREMS)

Vol. 02, Issue 10, October 2022, pp : 05-16

e-ISSN : 2583-1062

Impact Factor : 2.265

$$\sum_{e=1}^{n_e}\left[\bar{F}\right]^e\left\{\bar{P}\right\}^e=\sum_{e=1}^{n_e}\left[\left\{\bar{R}_H\right\}^e+\bar{\Omega}\left\{\bar{R}_H\right\}^e+\dot{\bar{X}}_j\left\{\bar{R}_{x_j}\right\}^e+\dot{\bar{Z}}_j\left\{\bar{R}_{z_j}\right\}^e\right] \quad (5)$$

$$\bar{F}_{ij}{}^e=\iint_{A^e}\bar{h}^{-3}\left[\frac{1}{12}\frac{\partial N_i\partial N_j}{\partial\alpha\partial\alpha}+\frac{1}{12}\frac{\partial N_i\partial N_j}{\partial\beta\partial\beta}\right]d\alpha d\beta \quad (6)$$

$$\bar{Q}_i^e=\int_{\bar{\Gamma}^e}\left\{\left(\frac{\bar{h}^3}{12}\frac{\partial\bar{p}^e}{\partial\alpha}-\frac{\bar{\Omega}\bar{h}}{2}\right)l_1+\left(\frac{\bar{h}^3}{12}\frac{\partial\bar{p}^e}{\partial\beta}\right)l_2\right\}N_i d\bar{\Gamma}^e \quad (7)$$

$$\bar{R}_{H_i}{}^e=\iint_{A^e}\frac{\bar{h}}{2}\frac{\partial N_i}{\partial\alpha}d\alpha d\beta \quad (8)$$

$$\bar{R}_{xj_i}{}^e=\iint_{A^e}N_i\cos\alpha d\alpha d\beta \quad (9)$$

$$\bar{R}_{zj_i}{}^e=\iint_{A^e}N_i\sin\alpha d\alpha d\beta \quad (10)$$

Where

$[\bar{F}]$= Assembled Fluidity Matrix

$\{\bar{P}\}$= Nodal pressure Vector

$\{\bar{Q}\}$= Nodal Flow Vector

$\{\bar{R}_H\}$ = Column Vectors due to hydrodynamic terms

$\bar{R}_{Zj}$ =Global right hand side vectors due to journal center linear velocities

l_1 & l_2 are the direction cosines and i,j =1,2.....n^e.

2.4. Boundary conditions

The following boundary conditions are applied in obtaining the solution of given problem

1. The nodes which are lying on the external boundary having zero pressure, p=0
2. The pressure at the trailing edge of positive region is zero, p = $\partial\bar{p}/\partial\alpha$=0.0
3. The pressure at leading edge is considered to be atmospheric, therefore p=0.0

Equation (5) can be solved to give pressure and flow simultaneously because at each node one of the two variables is known.

2.5. Journal center equilibrium position

For a given vertical external load or eccentricity ratio (ε) and operating and geometric parameters of the bearing, the journal center position ($\bar{X}j$, $\bar{Z}j$) is unique. This journal center equilibrium position is not known a priori and is obtained iteratively. Initially the tentative values of journal center coordinates ($\bar{X}j$, $\bar{Z}j$) are fed as input to compute the nominal fluid-film thickness ($\bar{h}$) that is required for the computation of fluid-film pressures. The fluid-film reaction components Fx and Fz are computed using Eqs. (11) and (12) respectively.

2.6 Performance characteristics

2.6.1. Static Performance Characteristics

The static performance characteristics of journal are computed for the steady-state condition ($\dot{\bar{x}},\dot{\bar{z}}=0$). It is essential to establish the journal center equilibrium position for the evaluation of performance characteristics at a given eccentricity ratio (ε).

Load carrying capacity ($\bar{F}_0$)

Fluid-film reaction components along X and Z directions are respectively given by [20]

$$\bar{F}_x=\int_{-\lambda}^{\lambda}\int_0^{2\pi}\bar{p}\cos\alpha d\alpha d\beta \quad (11)$$

$$\bar{F}_z=\int_{-\lambda}^{\lambda}\int_0^{2\pi}\bar{p}\sin\alpha d\alpha d\beta \quad (12)$$

www.ijprems.com
editor@ijprems.com

INTERNATIONAL JOURNAL OF PROGRESSIVE RESEARCH IN ENGINEERING MANAGEMENT AND SCIENCE (IJPREMS)

Vol. 02, Issue 10, October 2022, pp : 05-16

e-ISSN : 2583-1062

Impact Factor : 2.265

The resultant load carrying capacity is expressed as

$$\bar{L}_{cc} = \left[\bar{F}_x^{\,2} + \bar{F}_z^{\,2} \right]^{\frac{1}{2}} \tag{13}$$

Fluid-film frictional force (FL): The friction force in a journal bearing is computed from the following equation

$$\bar{F}_L = \sum_{e=1}^{n_e} \int_{A^e} \left(\frac{\bar{\Omega}\bar{\tau}_c}{\bar{h}} + \frac{\bar{h}}{2} \frac{\partial \bar{p}}{\partial \alpha} \right) \tag{14}$$

where

$\bar{\tau}_c$ is the normalized Couette shearing stress. For laminar flow, $\bar{\tau}_c$ =0

Coefficient of fluid-film friction can be calculated as

$$\bar{f} = \frac{\bar{F}_L}{L_{cc}} = f\left(\frac{R_j}{c} \right) \tag{15}$$

3. SOLUTION PROCEDURE

The numerical technique used in the present study for computing the optimum location of surface textures and then performance parameters of journal bearing is shown in Fig. 3. The exactness of theoretical solution depends on the mesh density and the simulated results should be independent of mesh density. Hence, a convergence study has been performed with various mesh densities to get mesh independent results. In the beginning the number of elements in circumferential direction is varied and elements in axial direction are fixed as 16 at first and the results are obtained at fixed value of eccentricity ratio as 0.5. It has been seen from Fig. 2(a) that the load carrying capacity increases with the number of elements in circumferential direction upto 63 and beyond 63 the load carrying capacity nearly stays constant. Also, it is seen from Fig. 2(b) that by increasing the number of elements in circumferential direction, the processing time increases drastically without any improvement in load carrying capacity. Similar procedure is adopted for choosing the number of elements in axial direction and decided as 20. Therefore to get work mesh independent and to limit computational time, the ideal mesh size has been chosen as 63 in circumferential direction and 20 in axial direction.

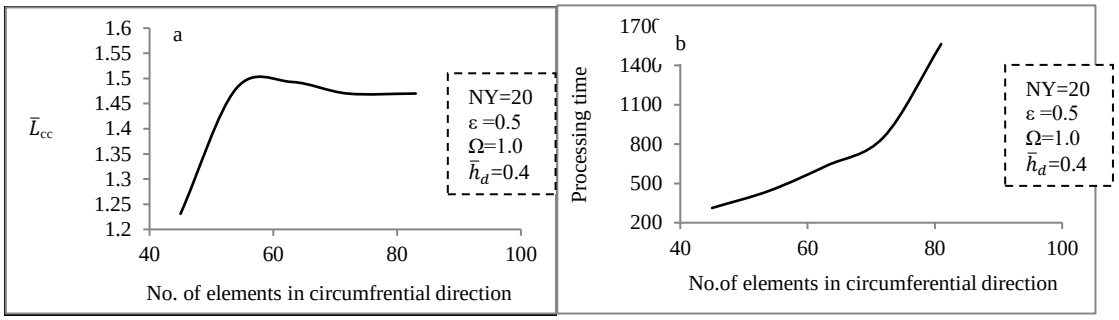

Fig.2: A convergence study of spherical textured journal bearing.

The numerical investigation of dimple/texture impact on the performance of journal bearing has been performed utilizing FEM and plan has been appeared in flow chart Fig.3. Following steps are associated with the solution procedure:

1.The fluid-film domain is discritized into four noded quadrilateral isoparametric elements by assigning number of elements in axial direction.

2. Fluid-film pressure field are initialised by assigning an arbitray value of journal center.

3.Fluid-film thickness is calculated for smooth and textured journal bearings.

4.A two point Gauss quadrature is used for the integration in elements. Thus four Gauss points are generated in an quadrilateral isoparametric elements.

5.Elements equations are assembled using indexing to obtain global system of matrices and then boundary conditions are implemented.

6.Newton's iterative method is used for establishing journal center.

7.Steps 2-6 are repeated until the equilibrium established and the pressure becomes positive and the given pressure convergence criteria is satisfied.

8.Once the pressure convergence criteria is satisfied and then static and dynamic performance characteristics are computed using the equations described above.

www.ijprems.com
editor@ijprems.com

INTERNATIONAL JOURNAL OF PROGRESSIVE RESEARCH IN ENGINEERING MANAGEMENT AND SCIENCE (IJPREMS)

Vol. 02, Issue 10, October 2022, pp : 05-16

e-ISSN : 2583-1062

Impact Factor : 2.265

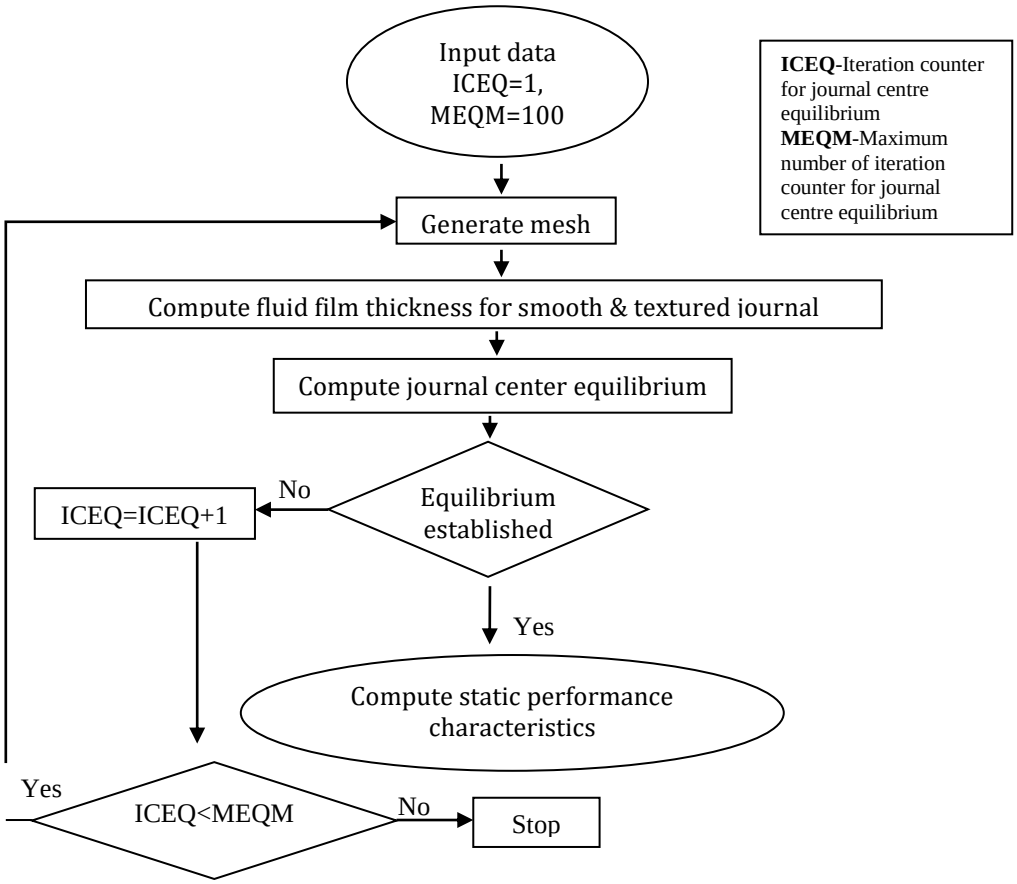

Fig.3 Flow chart of solution procedure

4. RESULTS AND DISCUSSION

In the present study, the spherical texture is used to investigate the effect of texture distribution on the journal bearing performance characteristics. The eccentricity ratio is equal to 0.3 (minimum loaded bearing).The textures are created on the bearing surface ranges from θ_1 to θ_2 in the circumferential direction and over the entire axial direction (Fig. 4). 9 cases are considered according to the geometric arrangement of textures on the bearing surface. The working and geometric parameters considered in this study are selected from the previously published work of Singh and Awasthi [20], shown in the Table 1.

Table 1: Working and geometric parameters used in the current study

Parameters	Non-dimensional value
Speed parameter ($\bar{\Omega}$)	1.0
Eccentricity ratio (ε)	0.3
Clearance ratio (C_r)	0.001
Aspect ratio (L/d)	1.0
Shape of micro-dimple	Spherical
No. of elements	1323
Area density of dimple (Sp)	51%
Dimple radius ($\bar{r}_p$)	0.16
Dimple depth ($\bar{h}_d$)	0.16
a	0.2
b	0.2
L_x	2a
L_z	2b

www.ijprems.com
editor@ijprems.com

INTERNATIONAL JOURNAL OF PROGRESSIVE RESEARCH IN ENGINEERING MANAGEMENT AND SCIENCE (IJPREMS)

Vol. 02, Issue 10, October 2022, pp : 05-16

e-ISSN : 2583-1062

Impact Factor : 2.265

4.1. Validation

In order to validate the developed MATLAB code for the computation of nodal pressure distribution and the performance characteristics parameters, the computed results are compared with the published work in Tables 2, 3 and 4. The computed value appears to be in good agreement with the published work.

Table 2: Comparison of Statics Characteristics of Plain Journal Bearing.

(Eccentricity Ratio ε=0.7, L/D=1.0, Grid size= 63×20)

Performance Parameters	Present Work	S.C. Jain et al. Ref. [23]	H.N. Chandrawat & R. Sinhasan Ref. [24]
Minimum Fluid-film Thickness ($\bar{h}_{\min}$)	0.300	0.300	0.300
Maximum Pressure ($\bar{P}_{\max}$)	5.480	5.360	5.516
Load Carrying Capacity	8.084	7.66	7.98
Attitude angle (Φ)	44.962	43.66	44.97
Friction coefficient ($\bar{f}$)	2.423	2.5457	2.4524

Table 4: Comparison of Statics Characteristics of Partially textured-I journal bearing

(Eccentricity Ratio ε=0.6, L/D=1.0, Grid size= 63×20)

Performance Parameters	Present Work	N. Tala-Ighil et al. Ref. [17]
Dimple depth ($\bar{h}_p$)	0.5	0.5
Angular location (θ˚)	195˚-230˚	185˚-230˚
Attitude angle (Φ˚)	50.48˚	49.0˚
Maximum Pressure (Pmax)	3.10	2.8

Load Carrying Capacity ($\bar{L}_{cc}$)

Figure 4 shows the variation of load carrying capacity ($\bar{L}_{cc}$) smooth/textured journal bearing versus texture location on the bearing surface in circumferential direction. It is noted that the load carrying capacity of partially textured has been improved maximum when the textures are created in the pressure built-up region ranging from θ_1=125° to θ_2=285° in the circumferential direction and over the entire axial direction vis-a-vis smooth journal bearing. Similar kinds of results are reported by Singh & Awasthi [20]. For a specific value of dimple depth 0.16, the percentage increase in the value of load carrying capacity is 8.19% as compared to smooth journal bearing.

Maximum fluid-film pressure ($\bar{P}_{max}$)

Figure 5 shows the variation of maximum fluid-film pressure ($\bar{P}_{max}$) of smooth/textured journal bearing versus texture location on the bearing surface in circumferential direction. It is noted that the maximum fluid-film pressure ($\bar{P}_{max}$) of partially textured journal bearing has been improved when the textures are created in the pressure built-up region ranging from θ_1=125° to θ_2=285° in the circumferential direction and over the entire axial direction vis-a-vis smooth journal bearing. Similar kinds of results are reported by Singh & Awasthi [20]. For a specific value of dimple depth 0.16, the percentage increase in the value of maximum fluid-film pressure ($\bar{P}_{max}$) is 18.64% as compared to smooth journal bearing.

Attitude angle (Φ)

Figure 6 shows the variation of attitude angle (Φ)of smooth/textured journal bearing versus texture location on the bearing surface in circumferential direction. It is noted that the value of attitude angle (Φ) of partially textured journal bearing is found minimum when the textures are created in the pressure built-up region ranging from θ_1=148° to θ_2=308° in the circumferential direction and over the entire axial direction vis-a-vis smooth journal bearing. It shows that the partially textured journal bearing is more stable if the textures are created in the zone (148°-308°). For a specific value of dimple depth 0.16, the percentage decrease in the value of attitude angle of textured journal bearing is 12.83% as compared to smooth journal bearing.

Lubricant end flow ($\bar{Q}$)

Figure 7 shows the variation of lubricant end flow ($\bar{Q}$) smooth/textured journal bearing versus texture location on the bearing surface in circumferential direction. It is seen that the value of lubricant end flow of partially textured is maximum when the textures are created in the pressure built-up region ranging from θ_1=125° to θ_2=285° in the

www.ijprems.com
editor@ijprems.com

INTERNATIONAL JOURNAL OF PROGRESSIVE RESEARCH IN ENGINEERING MANAGEMENT AND SCIENCE (IJPREMS)

Vol. 02, Issue 10, October 2022, pp : 05-16

e-ISSN : 2583-1062

Impact Factor : 2.265

circumferential direction and over the entire axial direction vis-a-vis smooth journal bearing. Similar kinds of results are reported by Singh & Awasthi [20]. For a specific value of dimple depth 0.16, the percentage increase in the value of load carrying capacity is 9.90% as compared to smooth journal bearing.

Fluid-film friction coefficient ($\bar{f}$)

Figure 8 shows the variation of fluid-film friction coefficient ($\bar{f}$) of smooth/textured journal bearing versus texture location on the bearing surface in circumferential direction. It is noted that the value of fluid-film friction coefficient ($\bar{f}$) of partially textured journal bearing is found minimum when the textures are created in the pressure built-up region ranging from θ_1=125° to θ_2=285° in the circumferential direction and over the entire axial direction vis-a-vis smooth journal bearing. It shows that the flow of the lubricant is ample in case of partially textured journal bearing if the textures are created in the zone (125°-285°). For a specific value of dimple depth 0.16, the percentage decrease in the value of fluid-film friction coefficient ($\bar{f}$) of textured journal bearing is 8.74% as compared to smooth journal bearing.

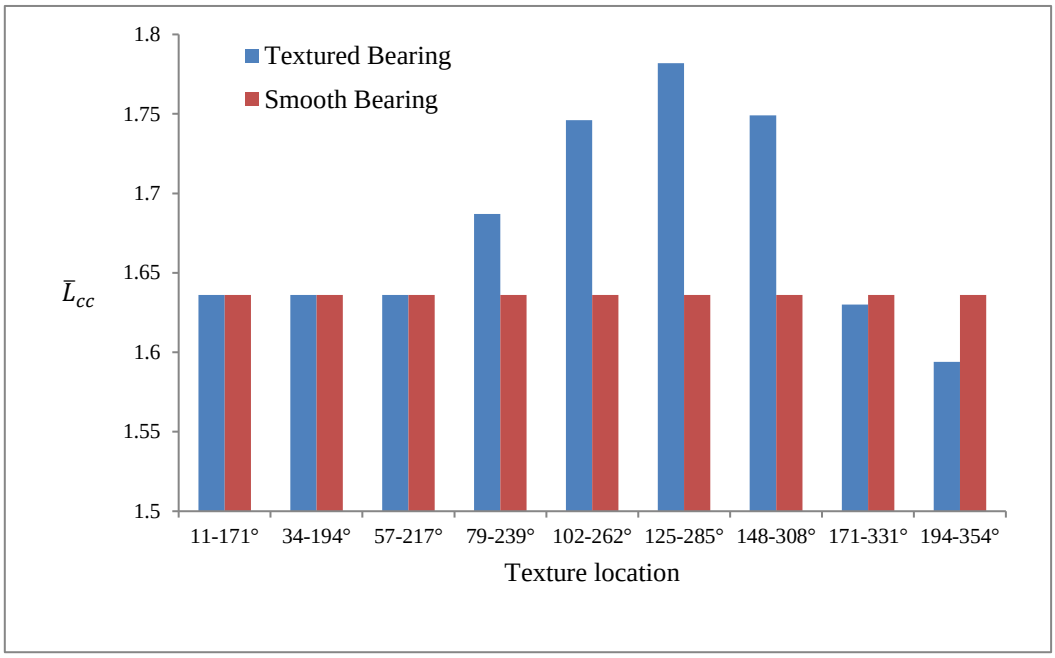

Figure 4: Load carrying capacity versus texture location in circumferential direction

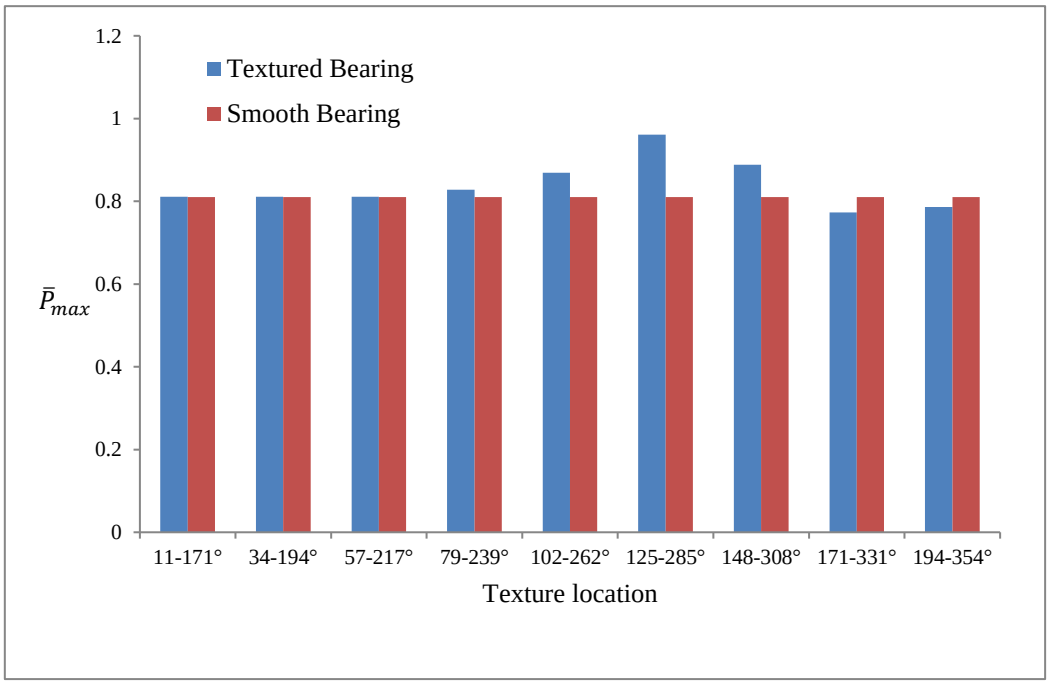

Figure 5: Maximum fluid-film pressure versus texture location in circumferential direction

www.ijprems.com
editor@ijprems.com

INTERNATIONAL JOURNAL OF PROGRESSIVE RESEARCH IN ENGINEERING MANAGEMENT AND SCIENCE (IJPREMS)

Vol. 02, Issue 10, October 2022, pp : 05-16

e-ISSN : 2583-1062

Impact Factor : 2.265

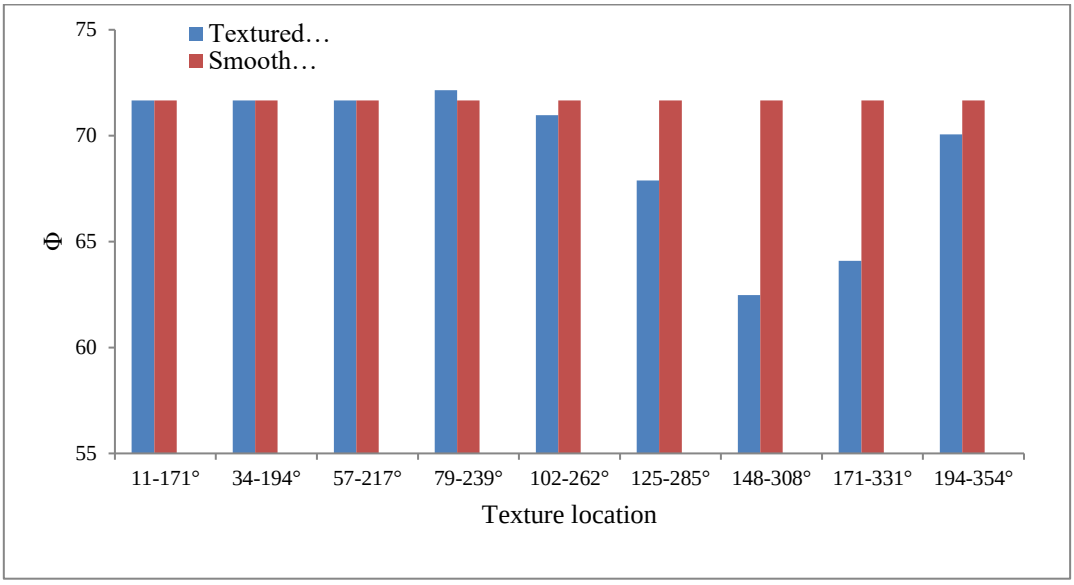

Figure 6: Attitude angle versus texture location in circumferential direction

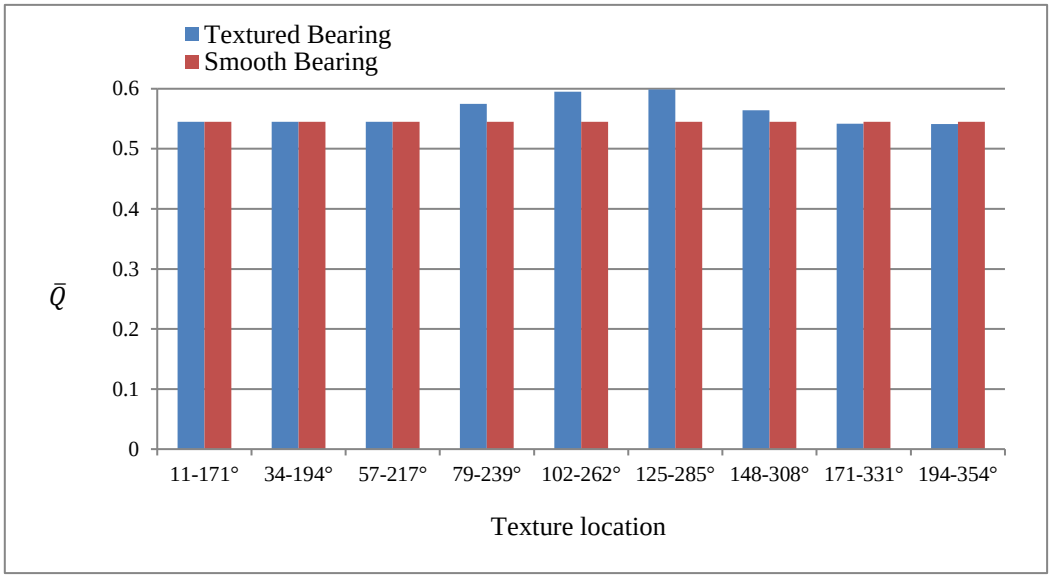

Figure 7: Lubricant end flow versus texture location in circumferential direction

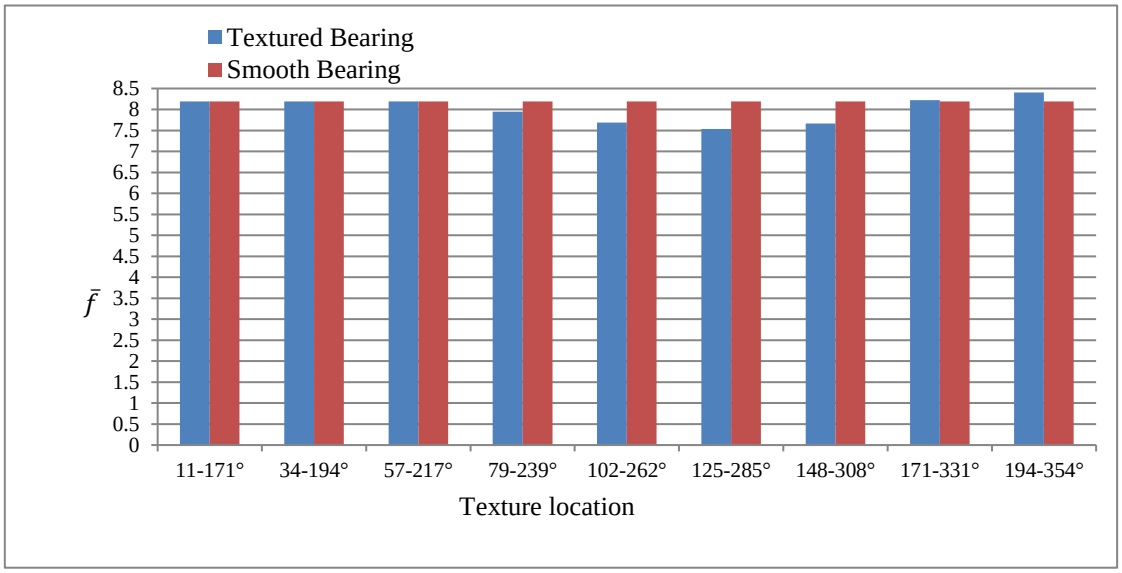

Figure 8: Fluid-film friction coefficient versus texture location in circumferential direction

www.ijprems.com
editor@ijprems.com

INTERNATIONAL JOURNAL OF PROGRESSIVE RESEARCH IN ENGINEERING MANAGEMENT AND SCIENCE (IJPREMS)

Vol. 02, Issue 10, October 2022, pp : 05-16

e-ISSN : 2583-1062

Impact Factor : 2.265

From the calculated results it is noted that the surface textures created on the bearing surface can improve the bearing performance characteristics. The most optimum results are obtained when the textures are created in the pressure build-up zone ranging from 125°-285° in the circumferential direction and over the entire axial direction. The most important static performance characteristics of journal bearing are shown in Table 5.

Table 5: Comparison of Statics Characteristics of Partially textured-I journal bearing

(ε=0.3, L/D=1.0, Grid size= 63×20, $\bar{h}_p = 0.16$)

Case	θ_1	θ_2	L_{cc}	P_{max}	Φ	$\bar{Q}$	$\bar{f}$
Smooth	-	-	1.636	0.810	71.667	0.545	8.192
1	11°	171°	1.636	0.811	71.67°	0.545	8.193
2	34°	194°	1.636	0.811	71.67°	0.545	8.193
3	57°	217°	1.636	0.811	71.67°	0.545	8.193
4	79°	239°	1.687	0.828	72.15°	0.575	7.95
5	102°	262°	1.746	0.869	70.97°	0.595	7.688
6	125°	285°	1.782	0.961	67.88°	0.599	7.533
7	148°	308°	1.749	0.888	62.47°	0.564	7.663
8	171°	331°	1.63	0.773	64.09°	0.542	8.219
9	194°	354°	1.594	0.786	70.06°	0.541	8.407

5. CONCLUSIONS

The current study presented the determination of optimum location of surface textures on the journal bearing surface. Also, the current shows the effect of textures on the bearing performance parameters. Following most important conclusions are drawn from the present work

1. The partial textures on the bearing surface can enhance the bearing performance parameters vis-a-vis smooth journal bearing.

2. The most optimum results are obtained when the textures are created in the pressure build-up region of 125°-285° on the bearing surface.

3. The optimum results are obtained when dimple aspect ratio is nearly unity.

NOMENCLATURE

Dimensional Parameters

C : Radial clearance, mm

D : Diameter of journal, mm

e : eccentricity of journal, mm

F : Fluid-film reaction$\left(\frac{\partial h}{\partial t} \neq 0\right)$, N

F_x, F_z : Fluid-film reaction components in X and Y direction$\left(\frac{\partial h}{\partial t} \neq 0\right)$, N

h : Nominal fluid-film thickness, mm

h_d : Dimple depth, mm

L : Bearing length, mm

L/D : Aspect ratio

N : Rotational speed, rpm

O_B : Bearing center

O_J : Journal center

p : Pressure, N/mm^2

p_s : Reference pressure, N/mm^2 $\left(\frac{\mu_r \omega_j R_j^{\,2}}{c^2}\right)$

R_j, R_b : Radius of journal and bearing, mm

S : Sommerfeld Number

www.ijprems.com
editor@ijprems.com

INTERNATIONAL JOURNAL OF PROGRESSIVE RESEARCH IN ENGINEERING MANAGEMENT AND SCIENCE (IJPREMS)

Vol. 02, Issue 10, October 2022, pp : 05-16

e-ISSN : 2583-1062

Impact Factor : 2.265

t : Time, sec

W : Load Capacity, N

W_0 : External load, N

x : Circumferential coordinate

y :Axial coordinate

X_j, Z_j : Coordinates of journal center

X, Y, Z: Cartesian coordinate system

z : Coordinate along film thickness

Non-Dimensional Parameters

$$\overline{F}_x, \overline{F}_z = \left(\frac{F_x}{p_s R_j^{\,2}}, \frac{F_z}{p_s R_j^{\,2}} \right)$$

$$\overline{h}, \overline{h}_{\min}, \overline{h}_d = \left(\frac{h}{c}, \frac{h_{\min}}{c}, \frac{h_d}{c} \right)$$

$$\overline{p} = \frac{p}{p_s}$$

$$\overline{p}_{\max} = \frac{p}{p_s}$$

$$\bar{Q} = Q \left(\frac{\mu}{c^3 p_s} \right)$$

$\overline{r}_p = \frac{r_p}{c}$, dimple radius

$$\overline{\tau}_c = t \left(\frac{c^2 p_s}{\mu_r R_j^{\,2}} \right)$$

$$\overline{W}_0 = \left(\frac{W}{p_s R_j^{\,2}} \right)$$

$$\overline{X}_j, \overline{Z}_j = \left(\frac{X_j}{c}, \frac{Z_j}{c} \right)$$

$$\overline{X}, \overline{Z} = \left(\frac{X}{c}, \frac{Z}{c} \right)$$

$$\alpha, \beta = \left(\frac{x}{R_j}, \frac{y}{R_j} \right)$$

$\varepsilon = \frac{e}{c}$, eccentricity ratio

$$\Omega = \omega_j \left(\frac{\mu_r R_j^{\,2}}{c^2 p_s} \right)$$

Greek Letters

μ : Lubricant viscosity, Pa. sec

α : Angular coordinate, radian

ω_{rad} : Angular speed, radian/sec

Φ : Attitude angle, radian

Subscripts and Superscript

b : Bearing

j : Journal

r : Reference value

min : Minimum value

Max :Maximum value : First derivative w.r.t. time

6. REFERENCES

[1] Priest M and Taylor C.M, "Automobile engine tribology-approaching the surface", Wear, vol.241, 2000, pp.193-203.

[2] Wakuda M, Yamauchi Y, Kanzaki S and Yasuda Y, "Effect of surface texturing on friction reduction between ceramic and steel materials under lubricated sliding contact", Wear, vol. 254, 2003, pp. 356-63.

[3] Kovalchenko O, Ajayi A, Fenske Erdemir G and Etsion I, "The effect of laser surface texturing on transitions in lubrication regimes during unidirectional sliding contact", Tribology International, vol. 38, 2005, pp. 219-25.

[4] Siripuram R.B and Stephens LS, "Effect of deterministic asperity geometry on hydrodynamic lubrication, Journal of Tribology, vol. 126, 2004, pp. 527-34.

[5] Dobrica M, Fillon M and Maspeyrot P, "Mixed EHD Lubrication in partial journal bearings-comparison between deterministic and stochastic models", ASME Journal of Tribology, vol. 128(4), 2006, pp. 778-88.

[6] Cupillard S, Glavatskih S and Cervantes M J, "Computational fluid dynamics analysis of journal bearing with surface texturing", Proceedings of the Institution of Mechanical Engineers, Part J: Journal of Engineering Tribology, vol. 222, 2008, pp. 97-107.

[7] Buscaglia GC, Ciuperca I and Jai M. The effect of periodic textures on the static characteristics of thrust bearings. Journal of Tribology 2005; 127: 899-902.

[8] Fowel M, Olver AV, Gosman AD, Spikes HA and Pegg I, "Entrainment and inlet suction: two mechanisms of hydrodynamic lubrication in textured bearings", Journal of Tribology, vol. 129, 2007, pp. 336-47.

[9] Brahamani R, Shirvani A and Shirvani H, "Optimization of partially textured parallel thrust bearings with square-shaped micro-dimples", Tribology Transactions, vol.50, 2007, pp. 401-6.

[10] Murthy AN, Etsion I, Talke FE, "Analysis of surface textured air bearing sliders with rarefaction effects", Tribology Letters, vol. 28, 2007, pp. 251-61.

[11] Tala-ighil N, Maspeyrot P, Fillon M and Bounif A, "Effects of surface texture on journal bearing characteristics under steady state operating conditions", Proceedings of the Institution of Mechanical Engineers, Part J: Journal of Engineering Tribology, vol. 221(6), 2007, pp. 623-34.

[12] Arghir M, Roucou N, Helene M and Frene J, "Theoretical analysis of the incompressible laminar flow in a macro-roughness cell", Journal of Tribology, vol. 125(2), 2003, pp. 309–18.

[13] Sahlin F, Glavatskikh S, Almqvist T and Larsson R, "Two dimensional CFD analysis of micro patterned surfaces in hydrodynamic lubrication", Journal of Tribology, vol. 127(1), 2005, pp. 96-102.

[14] De Kraker A, Ostryen RAJ, Van Beek A and Rixen D.J, "A multi scale method modelling surface texture effects", Journal of Tribology, vol. 129, 2007, pp. 221-30.

[15] Cupillard S, Glavatskih S and Cervantes M.J, "Pressure build up mechanism in a textured inlet of a hydrodynamic contact", Journal of Tribology, vol. 130(2), 2008, pp. 021701-10.

[16] Cupillard S, Glavatskih S and Cervantes M.J, "Inertia effects in textured hydro- dynamic contacts", Proceedings of the Institution of Mechanical Engineers, Part J: Journal of Engineering Tribology, vol. 224(8), 2010, pp. 751-756.

[17] Buscaglia GC, Ciuperca I and Jai M, "The effect of periodic textures on the static characteristics of thrust bearings", ASME Journal of Tribology, vol. 127, 2005, pp. 899-902.

[18] Buscaglia GC, Ciuperca I and Jai M, "On the optimization of surface textures for lubricated contacts", Journal of Mathematical Analysis and Applications, vol. 335, 2007, pp. 1309-27.

[19] Dobrica MB and Fillon M, "About the validity of Reynolds equation and inertia effects in textured sliders of infinite width", Proceedings of the Institution of Mechanical Engineers, Part J: Journal of Engineering Tribology, vol. 223, 2009, pp. 69–78.

[20] Singh N and Awasthi R.K, "Influence of dimple location and depth on the performance characteristics of the hydrodynamic journal bearing system", Proceedings of the Institution of Mechanical Engineers, Part J: Journal of Engineering Tribology, vol. 234(9), 2020, pp.1500-1513.

[21] Singh N and Awasthi R.K, "Influence of texture geometries on the performance parameters of hydrodynamic journal bearing", Proceedings of the Institution of Mechanical Engineers, Part J: Journal of Engineering Tribology, vol. 235(10), 2021, pp. 2056-2072.

[22] Singh N and Awasthi R.K, **"**Influence of surface textures on the dynamic stability and performance parameters of hydrodynamic two-lobe journal bearings**",** Proceedings of the Institution of Mechanical Engineers, Part J: Journal of Engineering Tribology, vol. 236(8), 2021, pp. 1589-1602.

[23] Jain S.C, Sinhasan R and Singh D.V, "A Study of EHD Lubrication in a Journal Bearing with Piezo-viscous lubricant", ASLE Trans. Vol. 27, 1984, pp. 168-176.

[24] Chandrawat H.N and Sinhasan R, "A Study of Steady State and Transient Performance Characteristics of Flexible Shell Journal Bearing", Tribology International, vol. 21, 1988, pp. 137-148.

[25] Tala-Ighil N, Fillon M and Maspeyrot P, "Effect of Textured Area on the Performance of Hydrodynamic Journal Bearing", Tribology International, vol. 44, 2011, pp. 211-219.